Skyrmions in a Doped Antiferromagnet

I. Raičević,[1,2] Dragana Popović,[1,2] C. Panagopoulos,[3,4] L. Benfatto,[5] M. B. Silva Neto,[6] E. S. Choi,[1] and T. Sasagawa[7]

[1]*National High Magnetic Field Laboratory, Florida State University, Tallahassee, Florida 32310, USA*
[2]*Department of Physics, Florida State University, Tallahassee, Florida 32306, USA*
[3]*Department of Physics, University of Crete and FORTH, 71003 Heraklion, Greece*
[4]*Division of Physics and Applied Physics, Nanyang Technological University, Singapore*
[5]*CNR-ISC and Department of Physics, "Sapienza" University of Rome, 00185 Rome, Italy*
[6]*Instituto de Física, Universidade Federal do Rio de Janeiro, CEP 21945-972, Rio de Janeiro - RJ, Brazil*
[7]*Materials and Structures Laboratory, Tokyo Institute of Technology, Kanagawa 226-8503, Japan*

(Received 4 June 2010; published 3 June 2011)

Magnetization and magnetoresistance have been measured in insulating antiferromagnetic $La_2Cu_{0.97}Li_{0.03}O_4$ over a wide range of temperatures, magnetic fields, and field orientations. The magnetoresistance step associated with a weak ferromagnetic transition exhibits a striking nonmonotonic temperature dependence, consistent with the presence of Skyrmions.

DOI: 10.1103/PhysRevLett.106.227206 PACS numbers: 75.47.Lx, 72.20.My, 75.50.Ee

A remarkable manifestation of complexity in magnetic systems is the emergence of topologically nontrivial arrangements of spins, such as Skyrmions [1]. These are "knots" in an otherwise ordered spin texture, which behave as excitations with particlelike properties. Skyrmions are stabilized by a magnetic field B in several ferromagnetic (FM) metals [2–5], where they manifest themselves in the electronic transport [2–4,6,7], or they form a detectable periodic Skyrmion lattice [5]. Skyrmions have been predicted to emerge also in the ground state of doped antiferromagnetic (AFM) insulators [8–10], but the identification of such isolated Skyrmions is a challenge. Neutron scattering, for example, would not be a definitive probe, since Skyrmions here do not form a lattice, while their possible signatures on transport may be screened by the insulating character of the carriers.

In a FM system, a charge carrier with the spin aligned to the magnetic background preserves its metallic character with a mass renormalization due to scattering by low-energy spin waves. Thus, the more complex spin excitations associated with topologically nontrivial magnetic textures have characteristic signatures in transport. This is indeed the case for Skyrmions in the polarized quantum Hall state of a two-dimensional electron gas [2,3], in colossal magnetoresistance (MR) manganites [4], and in the three-dimensional FM MnSi [6,7]. In a doped AFM insulator, the description of transport is complex already in the topologically trivial AFM ground state, since the carriers cannot move without inducing spin-flip scattering [8,11]. If, however, the external B field causes a change in transport that depends on the configuration of the spin background, the MR becomes a key probe to identify signatures of anomalous spin textures. This situation can be realized in the AFM insulator La_2CuO_4, lightly hole doped with Li. Here we show that the striking nonmonotonic temperature (T) dependence of the MR step associated with a B-induced magnetic transition is consistent with the Skyrmion formation.

La_2CuO_4, the parent material of $La_2Cu_{1-x}Li_xO_4$, is a Mott insulator with a residual AFM coupling between the $S = 1/2$ spins located at the Cu^{2+} ions, forming a nearly square lattice with a small orthorhombic distortion [12] [Fig. 1(a)]. A small antisymmetric Dzyaloshinskii-Moriya (DM) exchange between neighboring moments causes a uniform canting of the spins, leading to a weak ferromagnetism per CuO_2 plane, along with AFM ordering [Fig. 1(a)]. When La_2CuO_4 is doped with charge carriers, e.g., via Sr or Li substitution, the carriers frustrate the

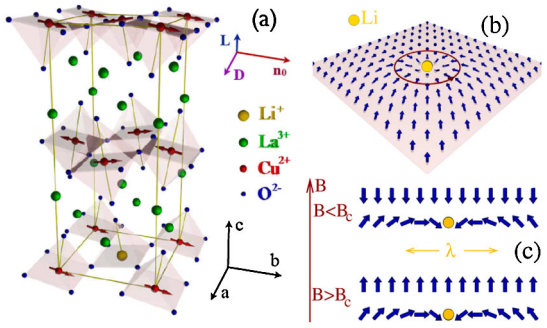

FIG. 1 (color online). (a) Orthorhombic crystal structure of La_2CuO_4; Li replaces Cu in CuO_2 (ab) planes. The spins on the Cu atoms have the AFM order with the large staggered component $\mathbf{n}_0$ along b and small FM components $\mathbf{L} = \mathbf{D} \times \mathbf{n}_0$ along c ($\mathbf{D}$, DM vector, aligned along a). The weak FM moments have staggered order along c at $B = 0$. (b) This AFM background becomes deformed near Li sites, via Skyrmion formation. For simplicity, we show the Skyrmion configuration of the FM moments only. The circle represents the Skyrmion core size λ. (c) Weak FM moments around the Li site across the weak FM transition: due to Skyrmion formation, spins have a FM order inside a distance of the order of λ at $B < B_c$ and AFM outside it, while the reverse is true for $B > B_c$.

magnetism, leading in both cases to a strong reduction of the Néel temperature T_N [13,14]. Different types of magnetic textures may be stabilized depending on the geometry and character of the dopants. For example, the diagonal incommensurate magnetic signatures reported by neutron-scattering experiments at very low (insulating) doping (x) [15] when Sr^{2+} replaces La^{3+} on top of a 4-Cu plaquette can be explained well by the formation of local spin spirals [8,16]. At higher x, the incommensurate magnetic signatures, now rotated by 45°, have been consistently attributed to the emergence of spin and charge stripes [17]. The substitution of Li^+ for Cu^{2+} in plane, on the other hand, may stabilize the formation of Skyrmions [10] that are obtained, roughly speaking, by reversing the average spins in a finite region of space around the dopant [Fig. 1(b)]. At low x, Skyrmions are expected to affect only the tails of NMR or neutron line shapes [10], making any unambiguous interpretation difficult, but even this has not been reported so far. Here instead we take advantage of the weak FM moments to tune the orientation of the AFM background using a uniform B. This gives rise to magneto-transport that is sensitive to the spin configuration around the dopants, and consequently to its nontrivial textures. The resulting MR data on AFM $La_2Cu_{0.97}Li_{0.03}O_4$ are consistent with the presence of local Skyrmions.

A high-quality $La_2Cu_{1-x}Li_xO_4$ (Li-LCO) single crystal with a nominal $x = 0.03$ was grown by the traveling-solvent floating-zone technique [18]. Magnetization M was measured in a standard superconducting quantum interference device magnetometer in $0.1 \leq B(\mathrm{T}) \leq 7$ applied either parallel or perpendicular to the CuO_2 (ab) planes. The in-plane resistance R was measured on a bar-shaped sample with dimensions $2.2 \times 0.57 \times 0.41$ mm^3 using a standard four-terminal ac method (~ 7 Hz) in the Ohmic regime. The contacts were made by evaporating Au and annealing at 700 °C in air. MR was measured by sweeping either $B \parallel ab$ or $B \perp ab$ at constant T in the 5–190 K range. The sweep rates were low enough to avoid the heating of the sample due to eddy currents.

In La-based AFM systems, the easy axis for the spins is the longest (b) of the two in-plane orthorhombic directions [19]. The DM vector $\mathbf{D}$ is oriented along a, the AFM order parameter $\mathbf{n}_0$ along b, so that the weak FM moments $\mathbf{L} = \mathbf{D} \times \mathbf{n}_0$ are parallel to c [Fig. 1(a)]. One signature of the presence of the weak FM moments is a peak in the magnetic susceptibility at T_N, such that it is more pronounced for $B \parallel c$ than for $B \parallel b$ [20,21]. This is indeed observed also in Li-LCO [Fig. 2(a)]. Since the sample is twinned, the B direction within the plane is not specified, but only twins having $B \parallel b$ contribute to anomalies in M (and resistivity ρ). T_N is suppressed by both $B \parallel c$ [Fig. 2(b)] and $B \parallel ab$ (not shown). Moreover, the low-T upturn of M is similar to that in undoped and Sr-doped La_2CuO_4 (LSCO) [21], and thus it is irrelevant to the Skyrmion formation. A second signature of the weak FM moments is found in $M(B)$ at fixed T. Because of the weak interplane AFM coupling, the weak FM moments have a

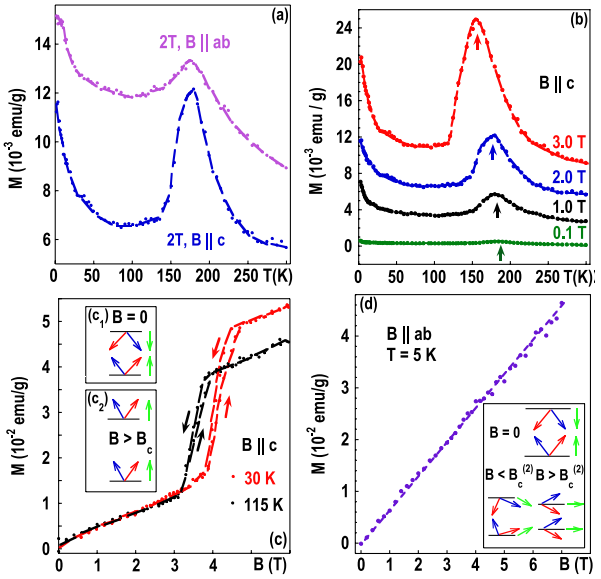

FIG. 2 (color online). (a) M vs T for $B \parallel c$ and $B \parallel ab$. The $B \parallel ab$ curve is shifted up by 3.5×10^{-3} emu/g. (b) M vs T for several $B \parallel c$. The curves at 1 and 0.1 T are shifted down by 1.5×10^{-3} emu/g and 1×10^{-3} emu/g, respectively. Arrows denote the Néel temperature; $T_N(B = 0) \approx 180$ K. (c) M vs $B \parallel c$ at different T. The arrows denote the direction of B sweeps. Insets: Spin configuration for (c_1) $B = 0$ and (c_2) $B > B_c$, where B_c is the critical field for the spin-flop transition [medium gray (red) and dark gray (blue) arrows, full Cu spins; light gray (green) arrows, weak FM moments]. (d) M vs $B \parallel ab$ at $T = 5$ K. Inset: Continuous rotation of spins in the bc plane for $B \parallel b$, where $B_c^{(2)}$ is the saturation field. Dashed lines guide the eye.

staggered order along the c axis [Fig. 2(c) inset (c_1)]. A sufficiently large field $B_c \parallel c$ can overcome the interplane AFM coupling and induce a discontinuous spin-flop reorientation in both the weak FM and the large AFM components [Fig. 2(c) inset (c_2)], causing the so-called weak FM (WFM), first-order transition [19,20,22]. This results in a jump $\Delta M(T)$ at $B_c(T)$ [22,23] [Fig. 2(c)]. Both $\Delta M(T)$ and $B_c(T)$ decrease with T [20,22,23], following the decrease of the staggered magnetization $n_0(T)$ due to thermal fluctuations [19]. For $B \parallel b$, the weak FM moments induce a continuous rotation of $\mathbf{n}_0$ in the bc plane [19,24] [Fig. 2(d) inset], so that $M(B)$ increases smoothly [Fig. 2(d)]. Thus the magnetic properties of Li-LCO resemble very much those of Sr- and O-doped La_2CuO_4 [20,21,23] where Skyrmions cannot form.

At very low x, the motion of the holes may be described as the hopping of (spinless) charges in the two AFM sublattices [8,11]. Because of orthorhombicity, the majority of holes have momenta close to $(\pi/2, -\pi/2)$ [25]; i.e., the most relevant pocket is the one along the b direction. When the Coulomb potential provided by the dopant is taken into account, the holes get localized, with a typical 2D pancakelike exponential envelope $\psi(r) \sim \exp(-r/\xi_0)$ (r, planar distance from the impurity site; ξ_0, localization length) [25]. The low-T electronic transport is then expected to occur via variable-range hopping (VRH) between

localized states [26] at a characteristic hopping distance $r_h(T)$. Indeed, the insulating behavior of R [Fig. 3(a)] follows a 2D VRH form $R \propto \exp(T_0/T)^{1/3}$ ($T_0 = 3753$ K) for $T < 23$ K, and it crosses over to $R \propto \exp(E_A/T)$ ($E_A = 313$ K) at higher T [27], similar to the behavior of other La-based AFM samples [12].

The in-plane MR $[R(B)/R(0) - 1]$ at first glance also resembles that of AFM LSCO [22,24]. For example, for $B \parallel ab$, the MR is negative, decreases continuously with a tendency to saturate above some threshold field [Fig. 3(b)], and its overall magnitude increases monotonically as T is reduced [Fig. 3(c)]. For $B \parallel c$, MR is also negative, with a steplike decrease [Fig. 3(d)] at the same critical field B_c where the WFM transition occurs and the uniform M shows a jump [Fig. 2(c)]. Moreover, both M [Fig. 2(c)] and MR [Fig. 3(d)] exhibit a hysteresis associated with a first-order phase transition. However, as shown below, it is the non-

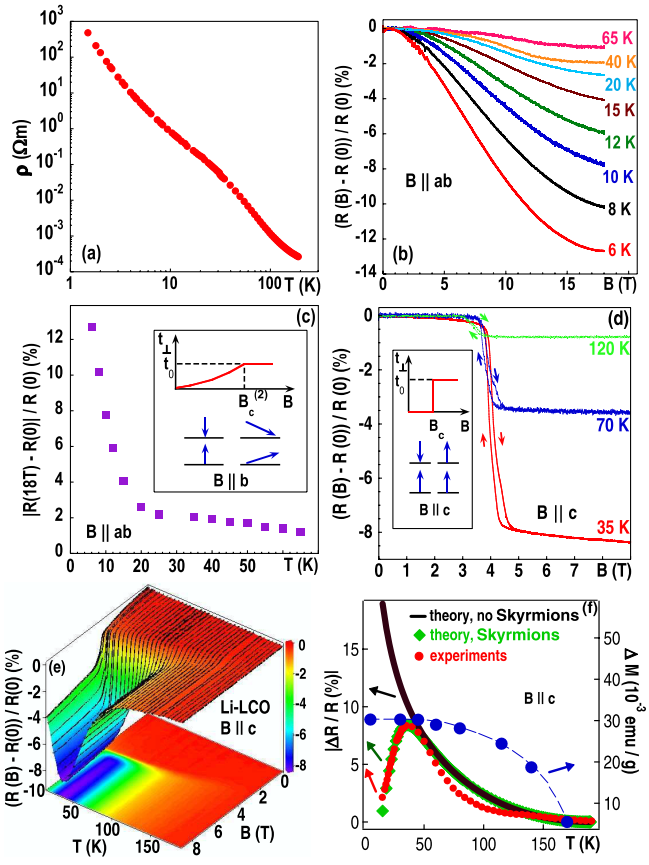

FIG. 3 (color online). (a) ρ vs T at $B = 0$. (b) MR for $B \parallel ab$ at several T. (c) MR vs T at 18 T for $B \parallel ab$. Inset: Sketch of the weak FM moments (blue arrows) and the corresponding interlayer hopping $t_\perp$ for $B \parallel ab$ (t_0, maximum value of $t_\perp$; $B_c^{(2)}$, saturation field). (d) MR for $B \parallel c$ at three selected T. Arrows denote the directions of the B sweeps. Inset: Weak FM moments (blue arrows) before and after the weak FM transition at B_c and the corresponding field-induced $t_\perp$. (e) MR for $B \parallel c$ at $15 \leq T(\mathrm{K}) \leq 190$. (f) The nonmonotonic T dependence of the MR step size shown in (e), and the monotonic decrease of the magnetization step with T. The dashed line guides the eye. The calculations of the MR step size in the presence and in the absence of Skyrmions [27] are also shown.

monotonic T dependence of the MR magnitude [Fig. 3(e)] and $|\Delta R|/R$ [Fig. 3(f)], the MR step size at B_c, that signals the formation of Skyrmions in the ground state of AFM Li-LCO. At high T, $|\Delta R|/R$ grows with decreasing T as expected, but unlike AFM LSCO [22], it exhibits a dramatic reversal of the behavior below $T \approx T_S = 35$ K, and starts to decrease as T is reduced further. We attribute this decrease to the progressive emergence of Skyrmions of increasing core size that suppress the interlayer tunneling process responsible for the negative MR in doped AFM La_2CuO_4 [25].

In general, holes can only tunnel between planes along the direction of FM order of the spins: b at $B = 0$ [Fig. 1(a)] and a above the WFM transition. However, since the hole momentum is close to $(\pi/2, -\pi/2)$ due to orthorhombicity, this hopping process is suppressed at $B = 0$. It becomes possible only above the WFM transition [27], modifying the in-plane wave function as $\psi_B(r) = f(r, B)\psi_0(r)$ ($\psi_{0,B}$ are the wave functions at zero and finite B, respectively). In the hopping-conductivity scheme described above, $R \sim |\psi(r_h)|^{-2}$, so that the MR is given by $\frac{R(B)-R(0)}{R(0)} = -(1 - \frac{|\psi_0(r_h)|^2}{|\psi_B(r_h)|^2})$. At the typical length scale $r_h(T)$ for hopping, $f(r_h, B) \simeq 1 + \alpha[r_h t_\perp(B)]^2 > 1$ [25], leading to a negative MR, as observed in Figs. 3(b), 3(d), and 3(e). Here $t_\perp$ is the interlayer hopping and $\alpha = 2/(\xi_0\epsilon_0)^2$ (ϵ_0, the localization energy of the hole bound state). When $B \parallel b$, $t_\perp(B) = t_0 \sin\theta(B)$ increases continuously with B [Fig. 3(c) inset]; here $\theta(B)$ is the angle with the b direction that spins form in their smooth rotation in the bc plane (see also Ref. [24]). However, for $B \parallel c$, $t_\perp(B)$ jumps discontinuously [Fig. 3(d) inset] from zero to the maximum value t_0 at the critical field B_c. Hence, the MR is continuous [24] for $B \parallel b$ [Fig. 3(b)], while it is discontinuous [22,23] for $B \parallel c$ [Fig. 3(d)].

In this picture, the T dependence of the step size $|\Delta R|/R$ is determined by $r_h(T)$ and $t_\perp(T)$. As the transport crosses over from the activated to the VRH regime [where $r_h(T) \sim \xi_0(T_0/T)^{1/3}$] at low T, $r_h(T)$ increases with decreasing T, and one expects only a monotonic increase of the MR magnitude. This is indeed observed for $B \parallel b$ [Fig. 3(c)] and in AFM LSCO [22]. Since the MR behavior is intimately related to the AFM order, any mechanism that leads to a global reduction of the AFM order parameter $n_0(T)$ may be expected to contribute also to a suppression of $|\Delta R|/R$. However, the low-T drop of $|\Delta R|/R$ cannot be ascribed to any such mechanism, since the magnetization step $\Delta M(T)$, which is proportional to $n_0(T)$ [19], increases continuously in the same T range [Fig. 3(f)]. This rules out, for example, spin glassiness, which is known to reduce $\Delta M(T)$ in AFM LSCO [28], but which here sets in only below 7–8 K [18]. It also rules out a structural change of the kind observed in $La_{1.79}Eu_{0.2}Sr_{0.01}CuO_4$ [29], although none have been reported on Li-LCO in our T range. Charge glassiness, which gives rise to a positive MR, is also not relevant, as it sets in at much lower T [30]. Thus the only mechanism that can lead to a decrease in $|\Delta R|/R$ is the local suppression of $t_\perp$, as it happens when a Skyrmion forms.

Close to the Li impurity position $r = 0$, where the Skyrmion is centered, $\mathbf{n}_0$ is nearly fully reversed with respect to the equilibrium direction and recovers only at distances $r \geq \lambda$ [λ, the characteristic length scale fixing the core size of the Skyrmion; Fig. 1(c)]. At $B = 0$, the ordering of spins in the two neighboring layers, the one with the impurity and the one above it, is nearly FM within a distance of the order of λ. For $B > B_c$, a full reversal of both weak FM and staggered moments occurs: the ordering of the magnetic moments within a distance λ from the impurity is AFM [Fig. 1(c)], and $t_\perp$ is suppressed for distances up to $r \simeq \lambda$. Thus, if the formation of Skyrmions suppresses $t_\perp$ in $f(r_h, B)$, the MR step size is expected to decrease. By modeling the gradual increase of λ as T is lowered [27], we have reproduced [Fig. 3(f)] the observed nonmonotonic behavior in $|\Delta R|/R$ for $B \| c$, characterized by a pronounced downturn below $T_S = 35$K. This behavior is contrasted to the smooth and monotonic increase in the case where no Skyrmions are formed [25]. Since λ obtained in our analysis is of the order of 1 lattice spacing [27], such nearly pointlike Skyrmions will interact very weakly among themselves and they are not expected to cause significant changes in bulk quantities, such as M. They will be crucial, however, in suppressing local processes, such as the vertical tunneling around the impurity, associated with the negative MR effect.

Skyrmions carry a nonzero topological charge, $Q \neq 0$, and a Skyrmion configuration is orthogonal to the $Q = 0$ Néel state. In order to stabilize a Skyrmion at $T = 0$, the hole state must modify the topology of the CuO_2 layers. Since the spins on the four nearest neighbors to the Li sites belong to the same AFM sublattice [Fig. 1(a)], the localized hole wave function can be labeled by the eigenvalues of the orbital angular momentum: $\ell = \pm 1$ (excited states) or $\ell = \pm i$ (lowest energy states) [9]. The $\ell = \pm i$ eigenstates have circulation associated with them, describing a localized hole orbiting around the Li center [9]. The associated, nonzero spin current induces the Skyrmion deformation of the AFM background [9,10]. This circulation might, or might not, be affected by an applied B, depending on whether the original symmetry of the problem is preserved. For $B \| c$, the symmetry is preserved, $\ell = \pm i$ are still good quantum numbers, and Skyrmions survive the applied B. For $B \| ab$, on the other hand, the symmetry is broken, the $\ell = \pm i$ states become mixed, causing the quenching of the hole angular momentum, and eventually Skyrmion formation is suppressed. As a result, $|\Delta R|/R$ increases monotonically as T is lowered [Fig. 3(c)], as expected without Skyrmion formation [see theory curve in Fig. 3(f)]. Such a monotonic increase is indeed observed in both $B \| ab$ and $B \| c$ for Sr doping [22], where Skyrmions cannot occur since the hole orbital angular momentum is always quenched, from the start, by the mixing between the two sublattices around the position of the Sr dopant. For vanishingly small $B \| ab$, however, Skyrmions might still be favorable and induce a nonmonotonic behavior for $|\Delta R|/R$, but probably for T much lower than those accessed in our experiment. Thus, what matters for the Skyrmion formation is the local structure of the hole wave function at the Sr or Li sites, not the way transport occurs. Indeed, in the AFM phase of interest, both LSCO [24] and Li-LCO show similar VRH or activated behavior, with differences emerging only at higher doping [13,14].

In summary, the low-T magnetic and transport properties of the AFM $La_2Cu_{1-x}Li_xO_4$ provide the first experimental support for the predictions of Skyrmions in AFM insulators. Our work may offer new insights into the mechanisms that can stabilize or suppress topological excitations in complex magnetic systems.

We thank X. Shi for technical help, V. Dobrosavljević, J. Lorenzana, A. N. Bogdanov for discussions, NSF DMR-0403491 and DMR-0905843, NHMFL via NSF DMR-0654118, MEXT-CT-2006-039047, EURYI, Italian MIUR Project PRIN-2007FW3MJX, and the National Research Foundation, Singapore, for financial support.

[1] A. N. Bogdanov *et al.*, Sov. Phys. JETP **68**, 101 (1989); C. Day, Phys. Today **62**, No. 4, 12 (2009).
[2] A. Schmeller *et al.*, Phys. Rev. Lett. **75**, 4290 (1995).
[3] D. K. Maude *et al.*, Phys. Rev. Lett. **77**, 4604 (1996).
[4] J. Ye *et al.*, Phys. Rev. Lett. **83**, 3737 (1999).
[5] S. Mühlbauer *et al.*, Science **323**, 915 (2009).
[6] A. Neubauer *et al.*, Phys. Rev. Lett. **102**, 186602 (2009).
[7] M. Lee *et al.*, Phys. Rev. Lett. **102**, 186601 (2009).
[8] B. I. Shraiman and E. D. Siggia, Phys. Rev. B **42**, 2485 (1990).
[9] R. J. Gooding, Phys. Rev. Lett. **66**, 2266 (1991).
[10] S. Haas *et al.*, Phys. Rev. Lett. **77**, 3021 (1996).
[11] C. L. Kane, P. A. Lee, and N. Read, Phys. Rev. B **39**, 6880 (1989).
[12] M. A. Kastner *et al.*, Rev. Mod. Phys. **70**, 897 (1998).
[13] A. I. Rykov *et al.*, Physica (Amsterdam) **247C**, 327 (1995).
[14] J. L. Sarrao *et al.*, Phys. Rev. B **54**, 12 014 (1996).
[15] M. Matsuda *et al.*, Phys. Rev. B **65**, 134515 (2002).
[16] A. Lüscher *et al.*, Phys. Rev. B **73**, 085122 (2006).
[17] S. A. Kivelson *et al.*, Rev. Mod. Phys. **75**, 1201 (2003).
[18] T. Sasagawa *et al.*, Phys. Rev. B **66**, 184512 (2002).
[19] L. Benfatto and M. B. Silva Neto, Phys. Rev. B **74**, 024415 (2006).
[20] T. Thio *et al.*, Phys. Rev. B **38**, 905 (1988).
[21] A. N. Lavrov *et al.*, Phys. Rev. Lett. **87**, 017007 (2001).
[22] Y. Ando, A. N. Lavrov, and S. Komiya, Phys. Rev. Lett. **90**, 247003 (2003).
[23] T. Thio *et al.*, Phys. Rev. B **41**, 231 (1990).
[24] S. Ono *et al.*, Phys. Rev. B **70**, 184527 (2004).
[25] V. N. Kotov *et al.*, Phys. Rev. B **76**, 224512 (2007).
[26] B. I. Shklovskii and A. L. Efros, *Electronic Properties of Doped Semiconductors* (Springer-Verlag, Berlin, 1984).
[27] See supplemental material at http://link.aps.org/supplemental/10.1103/PhysRevLett.106.227206 for more details.
[28] T. Suzuki *et al.*, Phys. Rev. B **66**, 172410 (2002).
[29] M. Hücker, Phys. Rev. B **79**, 104523 (2009).
[30] I. Raičević *et al.*, Phys. Rev. B **81**, 235104 (2010).